Hydromagnetics Natural Convection Stability of Liquid Metal in Inclined Cylindrical Annulus

Fateh MEBAREK-OUDINA*

Department of Physics, Faculty of Sciences, University of 20 août 1955 - Skikda,
B.P 26 Route El-Hadaiek, Skikda 21000, Algeria.
oudina2003@yahoo.fr, f.oudna@hotmail.com ; Phone: +213 668305488

Abstract

In this paper, natural convection stability of molten potassium in inclined cylindrical annulus under the influence of a radial magnetic field is investigated numerically. The top and bottom walls are thermally insulated, while the inner and outer cylinders are maintained at uniform temperatures. The inner and outer cylinders are maintained at isothermal but different temperatures, while the top and bottom walls are assumed to be adiabatic. The governing equations along with the boundary conditions are solved numerically using the finite volume method. SIMPLER and TDMA algorithms are used to find solution. The numerical results for various governing parameters of the problem at onset oscillatory state are discussed in terms of streamlines, isotherms and isobars in the annulus. These parameters are Hartmann number, inclination angle and radii ratio. The inclination and radii ratio of annulus have a significant effect on the stabilization of the magneto-convective flow, and shows that the best stabilization of oscillatory natural convection is obtained for strongest intensity of magnetic field, high radii ratio and at the inclination of the annulus $\gamma= 30°$.

Keywords: Magnetic field; Inclined cylindrical annulus; Natural convection; MHD stability; Numerical Simulation.

Nomenclature

A_r	aspect ratio = H/D (-)	$w*$	axial velocity, m.s^{-1}
B_0	magnetic field intensity, Tesla	u,w	dimensionless radial and axial velocities,
B_r	radial magnetic field, Tesla		respectively (-)
D	lengths (m)	**Greek symbols**	
F	Lorentz force, N.m^{-3}	α	thermal diffusivity of the fluid, m^2.s^{-1}
g	gravitational acceleration, m.s^{-2}	β	thermal expansion coefficient of the fluid, K^{-1}
H	height of enclosure, m	γ	inclination of annulus, °
Ha	number of Hartmann (-)	λ	radii ratio(-)
J	density of electric current, A.m^{-2}	κ	thermal conductivity, m^2/s
$\overline{Nu}$	number of average Nusselt (-)	ρ	fluid density, kg.m^{-3}
P	dimensionless pressure (-)	τ	time, s
Pr	number of Prandtl (-)	σ	electric conductivity, Ω^{-1}.m^{-1}
Ra	number of Rayleigh (-)	υ	kinematic viscosity of the fluid, m^2.s^{-1}
r^*,z^*	radial and axial coordinates, respectively	ψ	dimensionless stream function (-)
r_i,r_0	inner and outer radii, m	**Indices**	
t	dimensionless time (-)	Cr	criticize
Δt	increment of dimensionless time (-)	C	cold
T^*	temperature, K	EM	electromagnetic
T	dimensionless temperature (-)	H	hot
$u*$	radial velocity, m.s^{-1}	r,z	radial and axial directions, respectively

1. Introduction

Hydromagnetics or frequently used by the term of MHD is the dynamics of magnetic fields in the electrically conducting fluids such as liquid metals. Based on the know that conductive flow can support magnetic fields.

The investigation of magnetic field effects has important interest in the practical fields due its applications in engineering and industry. These applications include high temperature plasmas, cooling of nuclear reactors, MHD power generators, liquid metal flow control, micro MHD pumps, biological transportation, drying processes and solidification of binary alloy... etc. Hydromagnetics studies have a varied and wide application in channel and cavities, which explains the number of research found in this field with the consideration of different aspects.

In the present decades, problems of natural convection are the study object of many researchers. It is used by various industries as the design of heat exchangers and to make solar cells. Natural convection in a annular geometry are studied by some researchers such as Afrand *et al.* (2014a), Kakarantzas *et al.* (2014), Mebarek-Oudina and Bessaih (2016), Afsar Khan *et al.* (2016), Sankar *et al.* (2006)...etc

Kakarantzas *et al.* (2011) studied MHD natural convection of a melt in a vertical annulus with a flow driven by the volumetric heating and difference temperature in cylindrical annulus. The flow becomes laminar but loss their axisymmetry with the intensity of magnetic field.

Afrand *et al.* (2014b) in their investigation of fluid flow with the application of a magnetic field in an inclined cylindrical annulus, the overage Nusselt number decrease with the value of Hartmann number in the case where the magnetic field is perpendicular to the axis of annulus.

Teimouri *et al.* (2015) numerically investigated natural convection flow of molten potassium in a long horizontal annulus under the effect of radial magnetic field. The influence of magnetic field is reduced by the increasing of radii ratio.

Anil Lal *et al.* (2013) simulated the flow of natural convection inside a vertical cylindrical annulus closed at the top and opened at the bottom. A hot fluid is maintained below the open-end temperature while the outer cylindrical surface of the annulus is cooled to a low temperature. Their found that heat transfer through the annulus is subjected to sharp spatial variations. Also, the correlation for average Nusselt number and volume rate of flow is a function of Rayleigh number and percentage gap ratio.

Wrobel *et al.* (2010) experimentally and numerically analyzed convection in an annular enclosure with a round rod core and a cylindrical outer wall filled with paramagnetic fluid. They found that the magnetic field influences and yields heat transfer more efficiently than the thermal Rayleigh number.

Singh *et al.* (2012) analytically obtained the exact solutions for fully developed natural convection in open-ended vertical annuli under the effect of radial magnetic field. They showed the possibility of control the behavior of the fluid flow by the strength of the magnetic field and space between the cylinders. In another research, Singh *et al.* (1997) revealed that if the gap between cylinders is less than or equal to the radius of inner cylinder, the velocity and temperature of the fluid are higher in case of isothermal condition compared to constant heat flux case while reverse phenomena occur for the others gaps.

Sawada *et al.* (1993) experimentally investigated natural convection in concentric horizontal annuli containing magnetic fluid under varying magnetic fields. The effects of direction and the strength of magnetic fields are clarified. A wall-temperature distribution is observed when a magnetic field gradient is applied in the same direction as the gravity, while the reverse natural convection occurs if the magnetic field gradient is applied in the opposite direction of the gravity.

Metal cooled reactors usually use molten metals such as sodium, potassium or a combination of sodium and potassium for their immense heat transfer properties so that the reactor can be maneuvered at much higher temperatures and lower pressures. The aim of the present work is to investigate natural convection stability in an inclined annulus filled with molten potassium under radial magnetic field.

This numerical model is chosen for its various applications in the engineering and industry. The problem of nonlinear governing differential equations is solved by the finite volume method.

To our knowledge, the effect of inclinations of the cylindrical annulus on the oscillatory natural

convection under radial magnetic field has never been studied. The study is carried out in oscillatory state, for different cases: inclination of the annulus (γ= 0°, 30°, 60° and 90°), radii ratio, $\lambda \leq 6$ and under different intensity of radial magnetic field. The criticize Rayleigh number Ra_{Cr} and corresponding frequency, Fr_{Cr} associated with different inclination angles of annulus γ, radii ratio and Hartmann numbers are determined in each case and discussed. The paper is organized as follows: Section 2 presents the geometry and mathematical formulation. The numerical procedure used for the computation is given in Section 3 ; Section 4 discusses the grid effect and validation code; The results and discussion are available in Section 5. Finally, the conclusions are given.

2. Geometry & Mathematical Description

The geometry used in the present work is a cylindrical annulus formed by two cylinders of inner and outer radii, r_i and r_o, respectively as shown in Fig.1. The outer and inner cylinders are maintained at isothermal but different temperatures, T_C and T_H, respectively. The bottom and top walls are assumed to be adiabatic. The annulus is filled with a molten potassium (Pr = 0.072). The two-dimensional cylindrical coordinates (r, z) with their corresponding velocity components (u, w) are explicated in Fig.1. The inclination of the annulus is also considered, with a varying angle γ. It is necessary to note that in Fig.1, γ is the angle of incline, g is the gravity acceleration and B_0 is a uniform magnetic field, which is applied orthogonally to the r-direction. All walls are assumed to be electrically insulated. Also, we assume that the induced magnetic field produced by the motion of an electrically conducting fluid is negligible compared to the applied magnetic field B_0. By using D^2/υ, $D = r_0 - r_i$, υ/D, $T_H^* - T_C^*$, $\rho(\upsilon/D)^2$ as typical scales for time (s), lengths (m), velocities (m.s^{-1}), temperature (K) and pressure (N. m^{-2}), respectively. The equations governing Newtonian, viscous, steady, laminar, electrically conducting and incompressible fluid with Boussinesq approximation, after neglecting viscous and Ohmic dissipations in two-dimensional cylindrical co-ordinates (r, z), are written in dimensionless form as follows:
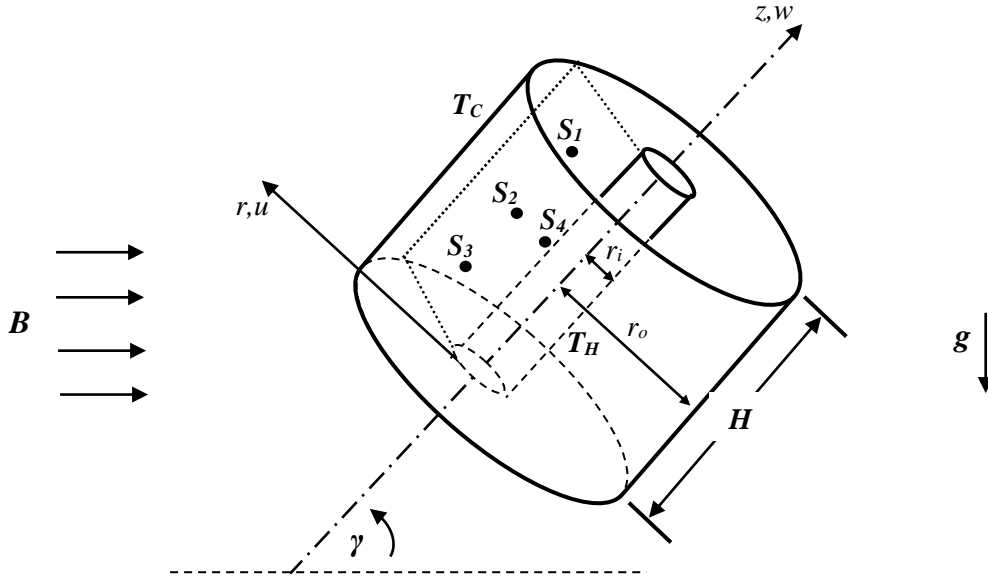
Fig. 1. Configuration of physical problem, S_1, S_2, S_3 and S_4 are local positions of the monitoring points.

Equation of dimensionless continuity:

$$\frac{1}{r}\frac{\partial(ru)}{\partial r} + \frac{\partial w}{\partial z} = 0 \qquad (1)$$

Equation of dimensionless momentum:
r-component

$$\frac{\partial u}{\partial t} + u\frac{\partial u}{\partial r} + w\frac{\partial u}{\partial z} = -\frac{\partial P}{\partial r} + \left(\frac{1}{r}\frac{\partial}{\partial r}\left(r\frac{\partial u}{\partial r}\right) + \frac{\partial^2 u}{\partial z^2} - \frac{u}{r^2}\right) +$$
$$\frac{1}{\Pr}\cdot Ra\cdot T\cdot\sin(\gamma) + F_{EMr} \qquad (2)$$

z-component

$$\frac{\partial w}{\partial t} + u\frac{\partial w}{\partial r} + w\frac{\partial w}{\partial z} = -\frac{\partial P}{\partial z} + \left(\frac{1}{r}\frac{\partial}{\partial r}\left(r\frac{\partial w}{\partial r}\right) + \frac{\partial^2 w}{\partial z^2}\right)$$
$$+ \frac{1}{\Pr}\cdot Ra\cdot T\cos(\gamma) \qquad (3)$$

3

Equation of dimensionless energy:

$$\frac{\partial T}{\partial t} + u\frac{\partial T}{\partial r} + w\frac{\partial T}{\partial z} = \frac{1}{Pr}\left(\frac{1}{r}\frac{\partial}{\partial r}\left(r\frac{\partial T}{\partial r}\right) + \left(\frac{\partial^2 T}{\partial z^2}\right)\right) \quad (4)$$

The dimensionless variables used in the present work are defined as follows:

$$t = \tau\Big/\frac{D^2}{\upsilon}\,,\; r = \frac{r^* - ri}{D}\,,\; z = \frac{z^*}{D}\,,\; u = u^*\Big/\left(\frac{\upsilon}{D}\right),$$

$$w = w^*\Big/\left(\frac{\upsilon}{D}\right),\; P = P^*\Big/\rho\left(\frac{\upsilon}{D}\right)^2,\; T = \frac{T^* - T_C^*}{T_H^* - T_C^*}$$

where F_{EMr} is the Lorentz force component in r direction, which is determined using the equation: F $= J \times B$, where B and J are the magnetic field and electric current vectors, respectively (Mebarek-Oudina & Bessaïh, 2014). The expression of this component is:

$$F_{EMr} = -Ha^2 \cdot u \quad (5)$$

The magneto convection problem in an cylindrical annulus is, therefore, governed by the following dimensionless parameters: $Ra = \frac{g\beta(T_H - T_C)D^3}{\nu\alpha}$ is the Rayleigh number, $Pr = \frac{\upsilon}{\alpha}$ is the Prandtl number, and $Ha = B_0 \cdot D\sqrt{\sigma/\rho\upsilon}$ the Hartmann number, which indicate the ratio of the electromagnetic forces to the viscosity forces. Here the Hartmann number is due to radial magnetic field, $\lambda = \frac{r_0}{r_i}$ the radii ratio and $A_r = \frac{H}{D}$ the aspect ratio.

where, $\alpha = \kappa/\rho C_p$ is thermal diffusivity of the liquid, κ is the thermal conductivity, C_p its specific heat to constant pressure, σ is the electrical conductivity and υ is the kinematic viscosity of the fluid.

The above equations are solved subject to the following initial and boundary conditions:

at $t = 0$, $u = w = T = 0$ (6)

for $t > 0$,

at $z = \frac{H}{D}$: $u = w = 0$, $\frac{\partial T}{\partial z} = 0$ Top adiabatic wall (7a)

at $z = 0$: $u = w = 0$, $\frac{\partial T}{\partial z} = 0$ Bottom adiabatic wall (7b)

at $r = 1$: $u = w = 0$, $T = 0$ Cold inner wall (7c)

at $r = 2$: $u = w = 0$, $T = 1$ Hot outer wall (7d)

The average Nusselt number at the hot cylindrical wall is expressed as:

$$\overline{Nu}\big|_{r=1} = \int_1^2 Nu \cdot dz \quad (8)$$

where, the local Nusselt number is $Nu = -\frac{\partial T}{\partial r}\Big|_{r=1}$

The stream function is defined as:

$$u = \frac{\partial \psi}{\partial z}\,,\; w = -\frac{\partial \psi}{\partial r} \quad (9)$$

3. Numerical Procedure

In this work, a FORTRAN computer code is developed and applied. The governing equations along with the boundary conditions are solved numerically using the finite volume method. The scalar quantities are stored at the center of control volume, while the vectorial quantities are stored on the faces of each volume.

The convection and diffusion terms in the governing equations are discretized with a second-order central difference scheme. The SIMPLER and TDMA algorithms are used to determine the pressure from continuity equation and to solve the coupled systems of discretized equations, respectively. (Patankar, 1980). The convergence is confirmed as soon as the maximum relative variation between two consecutive iteration levels fell below than 10^{-5}.

The irregular grid with the increments Δr and Δz are selected according to geometric progressions of ratio equal 1.07, to determine the specific characteristics of the magnetohydrodynamic flow and reduce numerical errors.

4. Grid effect and Validation

Various grid sizes are inspected to ensure grid independence results. The tested grids are demonstrated in Fig. 2. The results are achieved for inclined annulus with $A_r = 3$, $\lambda = 6.0$ and $\gamma = 30°$ containing low Prandtl number fluid, Pr = 0.072. Also, Rayleigh numbers and Hartmann are 10^7 and 40, respectively.

The grid independency tests are presented in Fig. 2 which includes the radial distribution of dimensionless temperature T at the middle of the annulus for different grids. We can see that the low relative error occurs between the two meshes 102 × 102 and 142 × 142. It does not exceed 2% indicated that it gives the same numerical solution of the problem. So, the grid used has 102×102 nodes. This grid is considered to show the greatest compromise between computational time and precision. Calculations are obtained by a PC with a 3 GHz CPU. Thus, the average computing time for a typical case is about 3 hours.
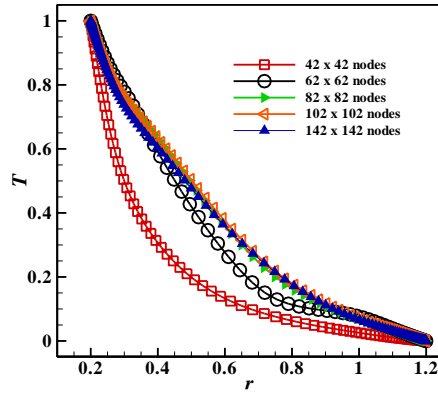
Fig. 2. Profiles of dimensionless temperature *T* with *r* at the middle of the annulus for different grids.
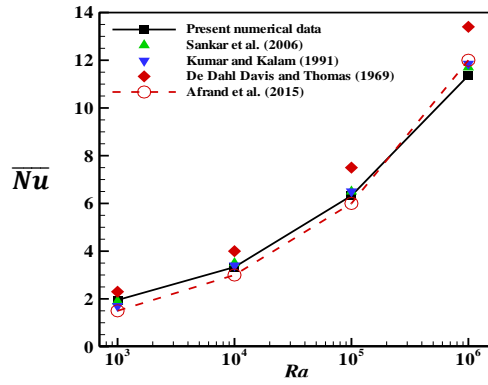
Fig. 3. Comparison of present results for heat transfer with data in the literature (A_r=1, λ=2 and $Pr = 0.7$).
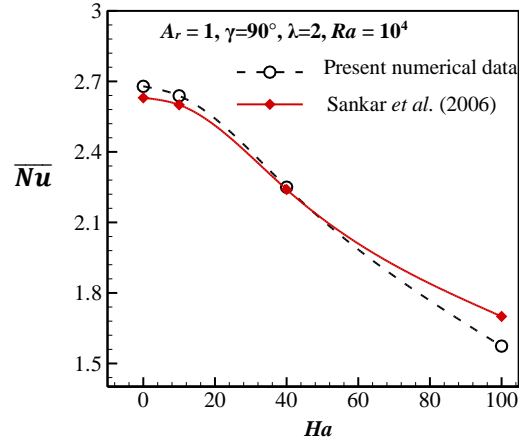
Fig. 4. Evaluation of Average Nusselt number via Hartmann number *Ha* for aspect ratio A_r=1, γ=90°, $Ra = 10^4$ and $Pr = 0.054$.
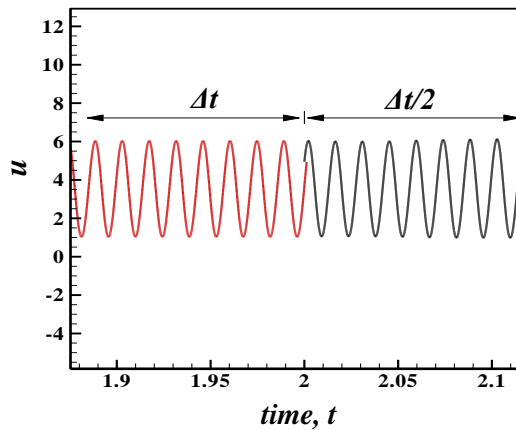
Fig. 5. Time evolutions of the dimensionless radial velocity, *u* at monitoring point S_3 and $\gamma = 30°$. Comparison is made between two time steps for $Ra_{Cr}= 4 \times 10^6$, λ=6 and $Ha = 0$.

In order to approve our numerical results, simulations of the present model are compared with the existing results accessible in the literature.

In the absence of magnetic field, the numerical results for different Rayleigh numbers are obtained. A good agreement is found between our numerical data and thus of De Dahl Davis and Tomas (1969), Kumar and Kalam's (1991), Sankar *et al*. (2006) and Afrand *et al*. (2015). The comparison is illustrated in Fig. 3, where the trend of the overall heat transfer rate increases with Ra, in the same manner with the approximated curves for all references.

In the presence of magnetic field, our code is validated with that of Sankar *et al*. (2006) and the comparison is presented in Fig. 4.

The heat transfer is suppressed by the application of magnetic field. From the equation (8), we can calculate the average local Nusselt number on the hot wall. With the increase of *Ha*, the value of Nusselt numbers decreases.

This result is the same to the result found by Sankar et al. (2006). Fig. 4 reveals a good agreement between our results and that of Sankar *et al.* (2006).

5. Results and Discussion

In this work, a numerical investigation of MHD natural convection stability of an electrically conducting fluid in an inclined cylindrical annulus with isothermally heated and cooled vertical walls and adiabatic top and bottom walls is presented. Simulations are carried out for value of Hartmann number ($0 \leq Ha \leq 80$), inclination angle ($0 \leq \gamma \leq 90$) and molten potassium ($Pr = 0.072$).

The annulus of radii ratio $\lambda = 6$, and aspect ratio $A_r = 3$ is applied in industries as well as the tubing industry, heat exchangers, power generation and the like. (Kakarantzas *et al.* (2011), Afrand *et al.* (2015))

5.1 Results without Magnetic Field

The origin of the instability is the interaction between the central vortex and the smallest vortices.

The major objective of the work is to detect the criticize Rayleigh number Ra_{Cr}, starting from which the flow becomes oscillatory. Successions of numerical calculations are carried out by increasing the Rayleigh numbers to obtain the physical instabilities, after the elimination of numerical instabilities. The oscillations amplitudes stay the same ones at two dimensionless time step Δt and $\Delta t/2$, for the physical instability. (Mebarek-Oudina, 2007)

Fig. 5 presents example of test Δt used in this study for Ha= 0, $\gamma = 30°$ and $\lambda=6$. The results of both dimensional time steps Δt, $\Delta t/2$ are in quite good agreement.

Fig. 6, shows the time evolution of the dimensionless temperature T, stream function ψ, radial velocity u and axial velocity w respectively at the probe S_3 for $Ra_{cr} = 4×10^6$ and $\gamma = 30°$. The flow oscillates in a simple periodic manner around the averaged values. All quantities used at this probe of the fluid domain are characterized by a particular signal. We note that the temporal resolution effects are investigated by using successive time steps until no differences are observed in the amplitude of oscillations. As expected, the amplitude of the dimensionless temperature T is smallest compared to other dimensionless quantities u, w and ψ.

The phase portraits are used during calculations to ensure that the amplitudes are uniform or, the sinusoidal character of temporal evolutions. Generally, they are used to inspect an intuitive and reliable of the movement regime.

Tories or phase portraits are closed loops with dominant harmonics, which means that the quasi-periodic flow regime is reached. The Fig. 7 presents the dimensionless velocity components in the phase planes (u,w) at the probe S_3 for $\gamma=30°$ and $\lambda=6$.

Thereby, the oscillatory character seen on the curves of time evolution is justified by the cyclical variation manner of the different parameters.

The oscillation frequency for the criticize value is determined using discrete Fourier transform of a certain number N, which has to be a power of 2. This transform is multiplied by the half of its conjugate quantity to obtain the power spectrum density (E) as a function of the oscillation frequencies F, defined by $F = M/(N\Delta t)$, where Δt is the dimensionless time step and M = 0, 1, 2...N/2. The values of E(F) represent several scales of sizes; in this case we use the decimal logarithm. Note that in this work, the peak of the energy spectrum, which corresponds to the major frequency F_{cr} for $N = 2^{16}$ and $\Delta t = 2 ×10^{-6}$ (Fig. 8), shows the criticize frequency of oscillations for this case of oscillatory flow, here equal to 69.33 (Mebarek-Oudina & Bessaih, 2014). In order to explain the nature of the flow oscillatory, we join the temporal evolution of the dimensionless radial velocity u at probe S_3 during one period with evolution of the flow structure (streamline and isotherm) at various dimensionless times: t_a, t_b and t_c, for $Ra_{cr} = 4×10^6$, $\gamma = 30°$, $\lambda = 6$ and Ha = 0 (Fig. 9). The flow field presents many cells. Size of these cells dilate and narrow gradually during the time (t_a, t_b and t_c).
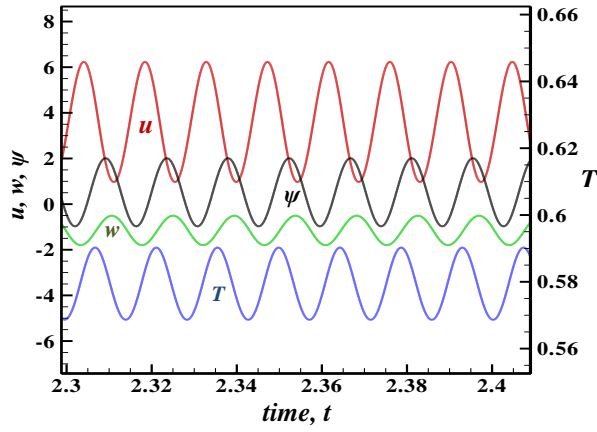
Fig. 6. Time evolution of the dimensionless temperature *T*, stream function *ψ*, dimensionless axial velocity component *w* and radial velocity component *u* at S_3 for $Ra_{cr} = 4 \times 10^6$, $\gamma = 30°$ and Ha = 0.
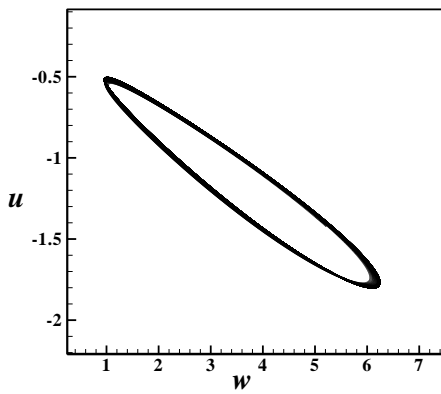
Fig. 7. Phase plot showing the variation between *u* and *w* for *Ha*= 0, *γ*=30°, *λ*=6, A_r = 3 and $Ra_{Cr} = 4 \times 10^6$.
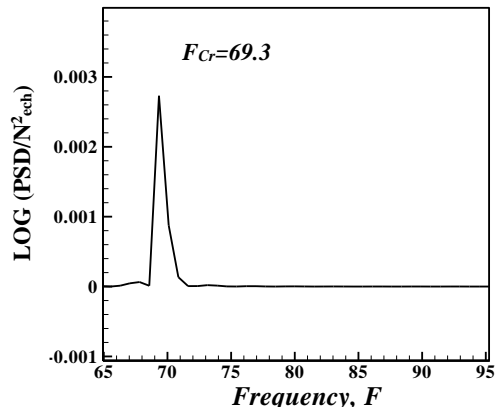
Fig. 8. Power spectrum of the dimensionless radial velocity component *u*, for $Ra_{Cr} = 4 \times 10^6$, *γ* = 30° and Ha = 0. Fr_{Cr} = 69.33, represent the dimensionless criticize frequency.
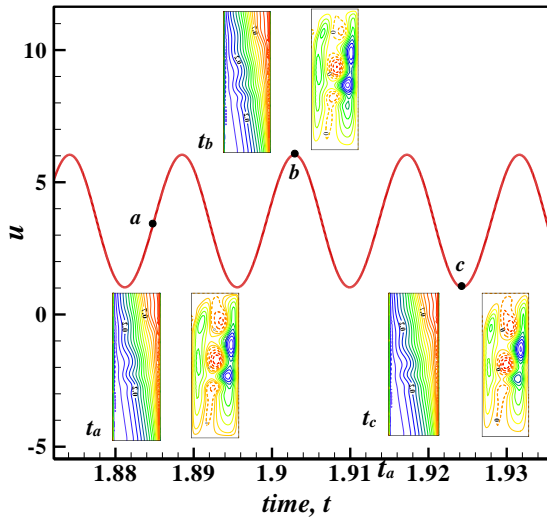
Fig. 9. Time evolution of the dimensionless radial velocity *u* in oscillatory flow at probe S_3, with streamlines and isotherms at various dimensionless time: t_a, t_b, and t_c for $Ra_{Cr} = 4 \times 10^6$, *Ha*=0 and *γ* = 30°.
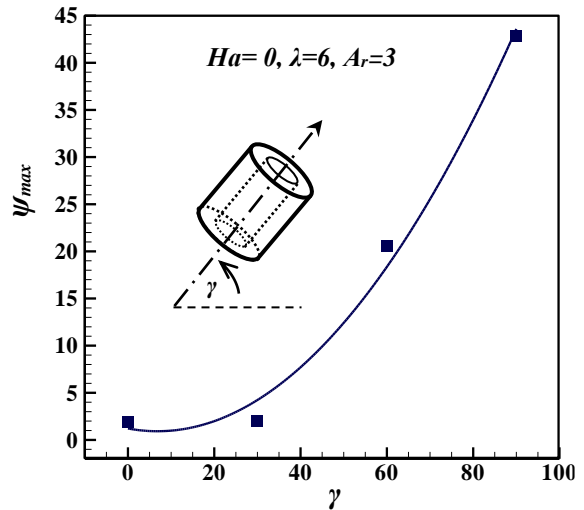
Fig. 10. Evolution of maximum stream function of the fluid via cavity inclination without magnetic field.

At time t_a, the structure characterized by recirculation cells (dashed lines) in middle with a positive mass flow and another secondary recirculation cells located at the two sides of the annulus. We note that, the streamlines structure at the time t_b is identical at the time t_c, which means that the oscillatory flow is periodic.

Variation of the maximum stream function of the fluid with cavity inclination for $\lambda=6$, $A_r=3$ and Ha=0 is shown in Fig. 10.

The effect of inclination on the stream function is clearly shown in this figure. This illustrates the relative insensitivity of the maximum stream function with inclination angle.

At different cavity inclination, the stream function ψ_{max} increases with inclination angles and it's the result of stronger buoyancy forces in the higher inclination of annulus.

5.2. Results with Magnetic Field

5.2.1. Effect of Magnetic Field

The magnetic field effect is introduced into the equations of momentum and potential through the Hartmann number. The radial magnetic field has a good ability to stabilize the convective flows, where the radial Lorentz force slows the velocity of particles.

To give the radial magnetic field effect on oscillatory flow in inclined cylindrical annulus, we are presented the evolution of criticize Rayleigh number and corresponding frequency for different Hartmann number with inclination angle of annulus, $\gamma = 30°$, $A_r=3$ and $\lambda = 6$, (Fig. 11). It can be seen that the variation of the Hartmann number have a significant effect on the stabilization of the flow. From this figure, the criticize Rayleigh number and its corresponding frequency increase, with the increase of Hartmann number.

It is clear that the best stabilization is found for strongest magnetic field, Ha = 80. Moreover, for all inclination angles the effect of the magnetic field on natural convection stability of fluid has almost the same trend.

5.2.2. Effect of Radii Ratio

At onset of oscillatory state of the flow detected for criticize Rayleigh number and fixed dimensionless time, the stream lines, isobars and isotherms for various values of λ, $Ha =40$ and $\gamma =30°$ are shown in Fig. 12.
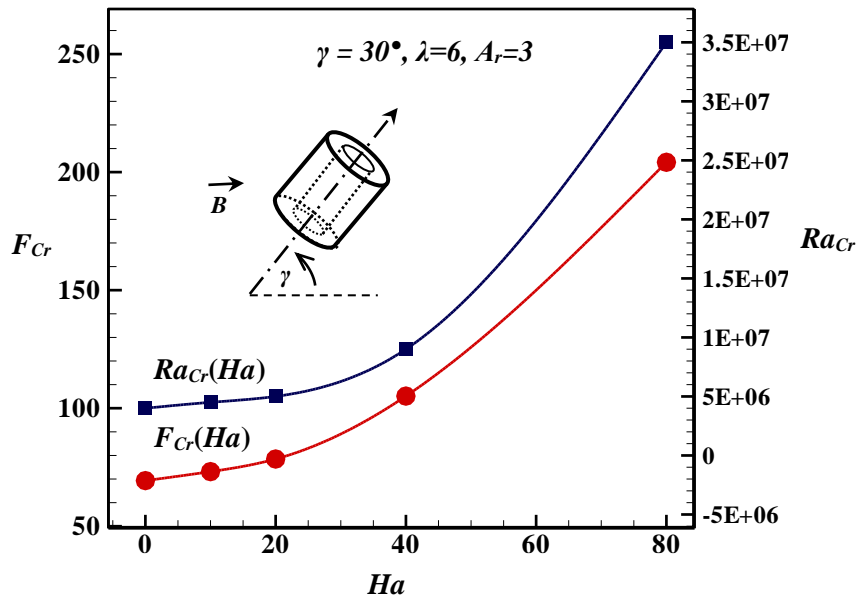
Fig. 11. Evolution of criticize Rayleigh number Ra_{Cr} and corresponding frequency Fr_{Cr} for different value of Hartmann number.

a) Isotherms, _T_

b) Isobars, _P_

c) Streamlines, _ψ_

λ=2   λ=4   λ=6
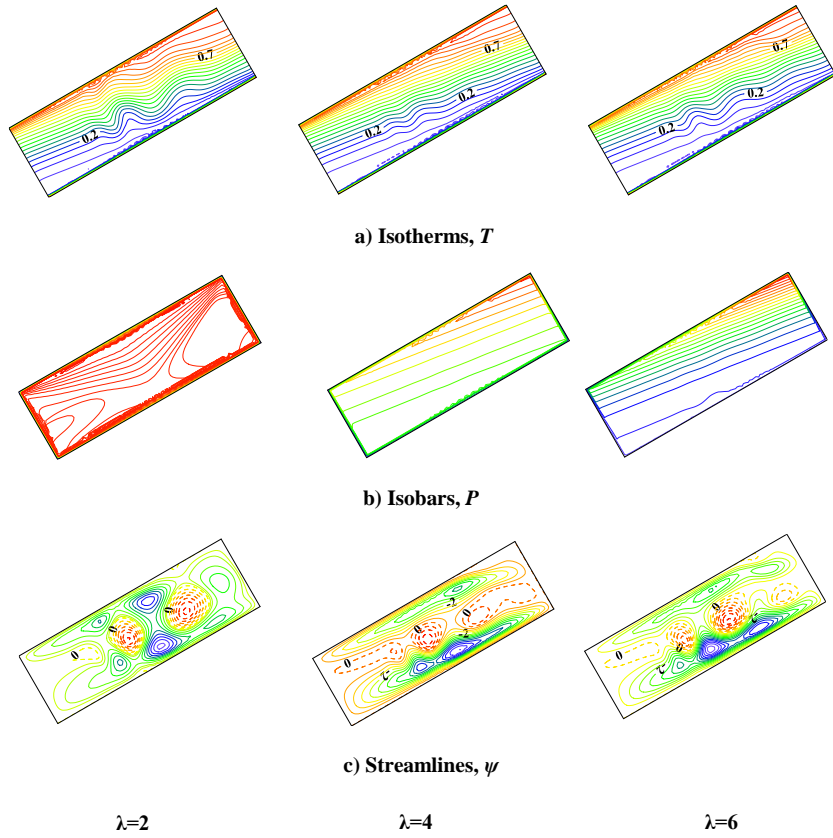
Fig. 12. Isotherms, isobars and streamlines for different radii ratio at onset oscillatory flow, t= 2, Ha= 40 and γ=30°.
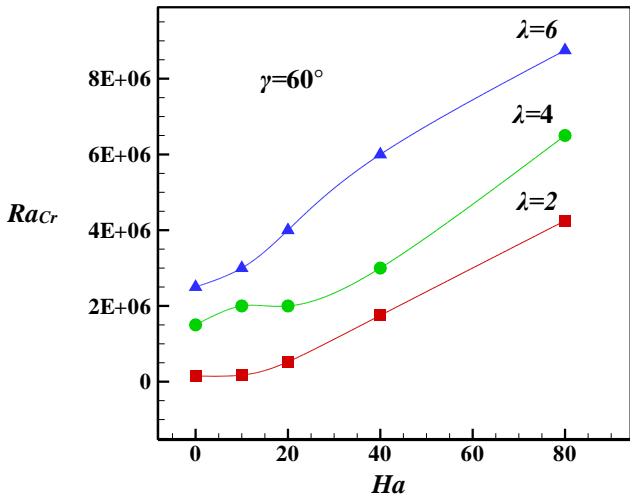
Fig. 13. MHD stability diagram (Ra_Cr − Ha) for different radii ratio and γ=60°.
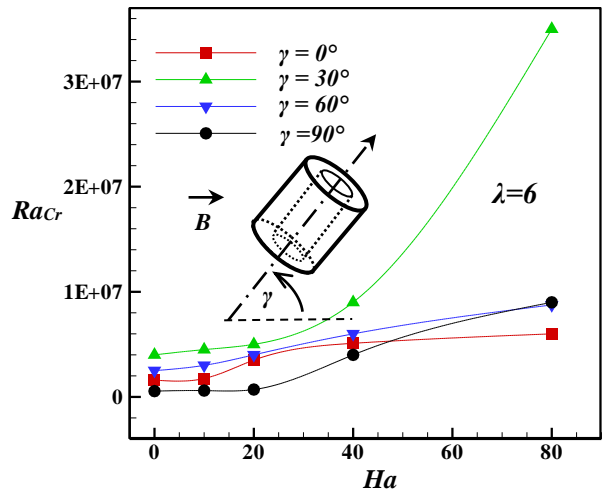
Fig. 14. MHD stability diagram (Ra_cr − Ha) for inclination angles and λ=6.
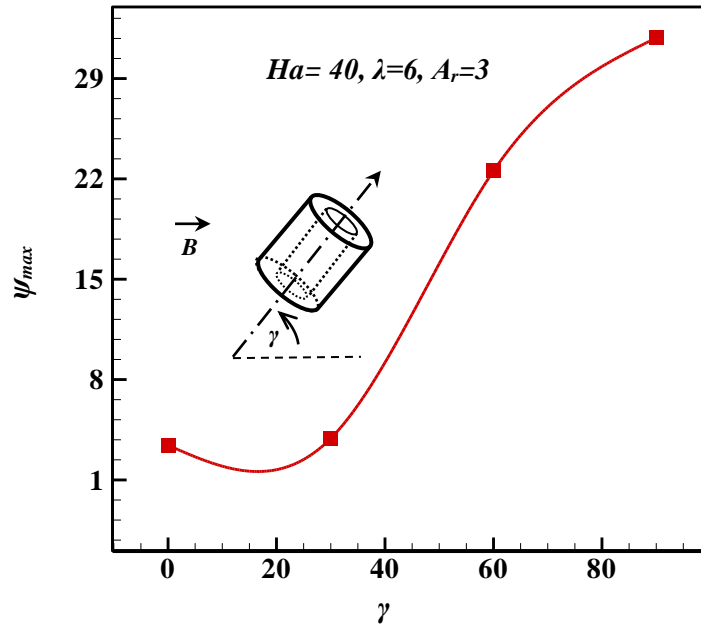
Fig. 15. Variation of the maximum stream functions of the fluid via the inclination angles of annulus and radial magnetic field.
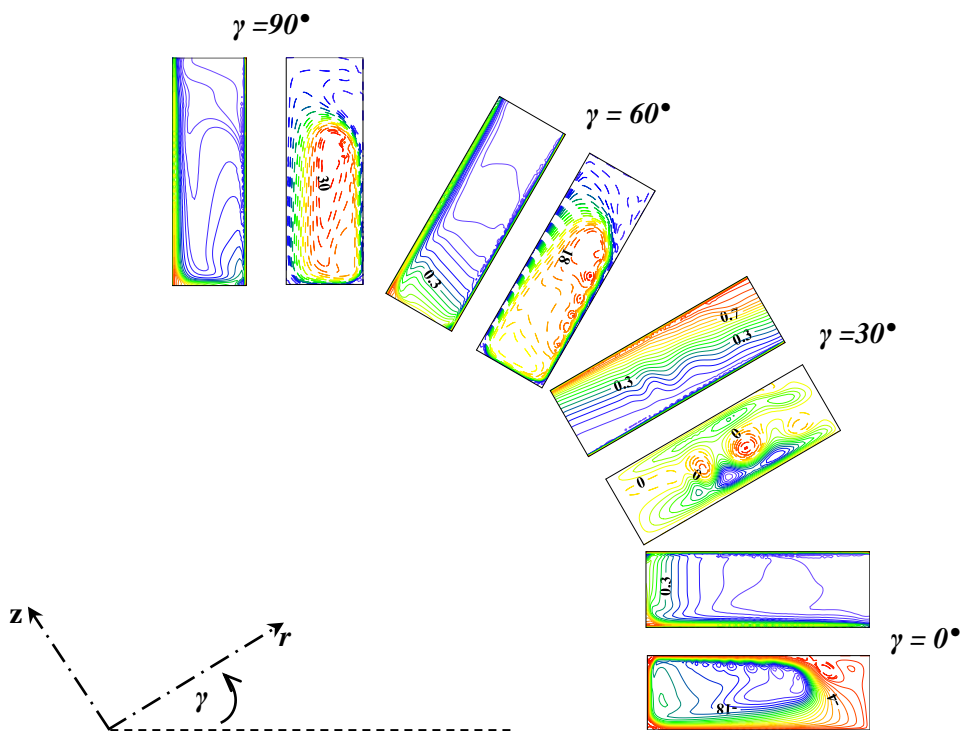
Fig. 16. Streamlines and isotherms at onset of instability for different inclination angles, $\lambda=6$, $A_r=3$ and $Ha = 40$.

Figure 12 shows the radii ratio effect on the flow patterns, isobars and isotherms in the annulus.
As shown by this figure for all radii ratios (λ), the isotherms are parallel with few deformations for each radii ratio. The pressure is low on the right of annulus, and high at left. Lines at constant pressure are approximately vertical in both cases. At certain point, pressure gradients are high and capable of overcoming buoyancy; the flow is separated to create the secondary vortex cells.
With the increase of radii ratio (λ), the isobar lines become parallel and the value of isobars decrease.

10

The natural convection is reduced by the application of stronger magnetic field and/or with the increasing of radii ratio.

Also, for each radii ratio the flow is characterized by a special stream lines. In this figure the results are presented and arranged in order to demonstrate clearly the effect of radii ratio. Figure 13, presents a stability diagram (Ra_{Cr}-Ha) for various values of radii ratio and inclination angle of the annulus γ =60°, it is clear that the best stabilization is found for higher radii ratio, λ = 6, for all Hartmann numbers used in this investigation.

With a good observation of this stability diagram, we remark that the radii ratio is more effective to stabilize the flow than the intensity of the magnetic field.

With increasing radii ratio, the effect of magnetic field on natural convection reduces.

For example; the value of Ra_{Cr} for λ= 2 and Ha ≤ 40 is inferior or of the order to that for λ = 4 without magnetic field.

From Fig. 13, the best stabilization is found for higher radii ratio and strongest magnetic field.

5.2.3. Effect of inclination angles

In this case, the results are arranged and presented in order to demonstrate clearly the effect of inclination angles.

Figure 14, shows a comparison between the case of different inclination angles, radii ratio λ = 6 and radial magnetic field (Ha= 0, 10, 20, 40 and 80). It is clear that the best stabilization is found where the inclination of annulus equals a γ= 30°.

For all inclination angles of annulus, the increasing of criticize Rayleigh number with the values of Hartmann number. This growth is very clear for the case of γ= 30°.

Variation of the maximum stream function of the fluid with cavity inclination for *λ=6, A_r=3* and Ha=40 is shown in Fig. 15. The same result found without magnetic field is obtained with the application of magnetic field. Furthermore, for all radii ratio and Hartmann numbers, the effect of the maximum stream function on the inclination angles of annulus has almost the same trend.

Fig. 16 shows clearly the effect of inclination angles of annulus for isotherms and streamlines. At onset of oscillatory instability, Ha= 40 and λ=6, the isotherms and streamlines distributions are presented at various inclination angles from γ = 0° to γ = 90°.

Inspection of isotherms in various inclination angles makes it clear, the isotherms are perpendicular at γ = 0° and 60°, parallels with few deformations for γ = 30° and parallels with an persistent deformations for 90°. The isotherms show how the motion is driven.

With the presence of radial magnetic field (Ha = 40), the temperature field is very significant. Fig. 16 shows the existence and the predominance of the convective mode compared to the diffusive mode for γ = 0°, 60° and 90° (deformation of the isotherms).

The iso-contours pattern of dimensionless stream function is characterized by one large cell with positive quantities for γ = 90° and 60°, and negative quantities for γ = 0°. For γ = 30°, two small cells with positive quantities appear in the middle of annulus.

In the center of cells locates the maximum and minimum lines of stream function. With the increase of inclination angles, the maximum stream line increases.

6. Conclusion

A computer code is applied to study the MHD natural convection processes in cylindrical annulus cavity. The effect of the criticize Rayleigh number, the Hartmann number, inclination angles of annulus and the radii ratio are investigated and the following results are achieved:

- The natural convection stability inside the annulus depends strongly on the radii ratio, strength of the magnetic field, inclination angles, and criticize Rayleigh number;
- The best stabilization is found for the inclination angle of annulus, γ= 30°;
- With the increasing of radii ratio, the value of isobars decrease;
- The increasing of the criticize Ra numbers and corresponding frequencies with the values of the Hartmann number. For various inclination angles, radii ratios and the magnetic field directions used in this study, the magnetic field has a stabilizing effect for this kind of flow;
- The increase of radii ratio is more effective to stabilize the flow than the intensity of the magnetic field;
- For all cases, the stream function ψ_{max} increases with inclination angles;
- The best stabilization of oscillatory natural convection is obtained for strongest intensity of magnetic field, high radii ratio and at the inclination of the annulus γ= 30°.

References

Afrand M., Sina N., Teimouri H., Mazaheri A., Safaei M. R., Esfe M. H., Kamali J. and Toghraie D. (2015) "Effect of Magnetic Field on

Free Convection in Inclined Cylindrical Annulus Containing Molten Potassium," *International Journal of Applied Mechanics* 7 (4) 1550052.

Afrand, M., Farahat, S., Hossein Nezhad, A., Sheikhzadeh, G.A., Sarhaddi, F. (2014a) "Numerical simulation of electrically conducting fluid flow and free convective heat transfer in an annulus on applying a magnetic field," *Heat Trans Res* 45, 749–766.

Afrand, M., Farahat, S., Nezhad, A.H., Ali Sheikhzadeh, G., Sarhaddi, F. (2014b) "3-D numerical investigation of natural convection in a tilted cylindrical annulus containing molten potassium and controlling it using various magnetic fields," *International Journal of Applied Electromagnetics and Mechanics*, 46, 809-821.

Anil Lal, S., & Arun Kumar, V. (2013) "Numerical Prediction of Natural Convection in a Vertical Annulus Closed at Top and Opened at Bottom," *Heat Transfer Engineering*, 34 (1), 70-83.

Afsar Khan, A., Sohail, A., Rashid, S., Rashidi, M.M., Alem Khan, N. (2016) "Effects of slip condition, variable viscosity and inclined magnetic field on the peristaltic motion of a non-Newtonian fluid in an inclined asymmetric channel", *Journal of Applied Fluid Mechanics*, 9 (3), 1381-1393.

De Vahl Davis, G., & Thomas, R.W. (1969) "Natural Convection Between Vertical Cylinders. In High speed computing in fluid dynamics," *Phys. Fluids* (Supplement-II), 198–207.

Kakarantzas, S. C., Sarris, I. E., & Vlachos, N. S. (2014) "Magnetohydrodynamic Natural Convection of Liquid Metal Between Coaxial Isothermal Cylinders Due to Internal Heating," *Numerical Heat Transfer, Part A* 65,401–418.

Kakarantzas, S.C., Sarris, I.E., Vlachos, N.S. (2011) "Natural convection of liquid metal in a vertical annulus with lateral and volumetric heating in the presence of a horizontal magnetic field," *Int. J. Heat Mass Transfer* 54, 3347–3356.

Kumar, R., & Kalam, M.A. (1991) "Laminar Thermal Convection Between Vertical Coaxial Isothermal Cylinders," *Int. J. Heat Mass Transfer*, 34 (2), 513–524.

Mebarek-Oudina, F., Bessaïh, R. (2007) "Magnetohydrodynamic Stability of Natural Convection Flows in Czochralski Crystal Growth," *World Journal of Engineering* 4 (4), 15–22.

Mebarek-Oudina, F., Bessaïh, R. (2014) "Numerical modeling of MHD stability in a cylindrical configuration," *Journal of the Franklin Institute* 351 (2), 667–681.

Mebarek-Oudina, F., Bessaïh, R. (2016) "Oscillatory Magnetohydrodynamic Natural Convection of Liquid Metal between Vertical Coaxial Cylinders, *Journal of Applied Fluid Mechanics* 9 (4), 1655-1665.

Patankar, S.V. (1980) *Numerical Heat Transfer and Fluid Flow* (McGraw-Hill, New-York).

Sankar, M., Venkatachalappa, M., Shivakumara, I.S. (2006) "Effect of magnetic field on natural convection in a vertical cylindrical annulus," *International Journal of Engineering Science* 44 (20), 1556–1570.

Sawada, T., Kikura, H., Saito, A., Tanahashi, T. (1993) "Natural convection of a magnetic fluid in concentric horizontal annuli under nonuniform magnetic fields," Exp. Thermal Fluid Sci. 7, 212–220.

Singh, R.K., Singh, A.K. (2012) "Effect of induced magnetic field on natural convection in vertical concentric annuli," *Acta Mech. Sin.* 28, 315–323.

Singh, S. K., Jha, B. K. and Singh, A. K. (1997) "Natural convection in vertical concentric annuli under a radial magnetic field," *Heat and Mass Transfer* 32, 399–401.

Teimouri, H., Afrand, M., Sina, N., Karimipour, A. and Isfahani, A. H. M. (2015) "Natural convection of liquid metal in a horizontal cylindrical annulus under radial magnetic field," *International Journal of Applied Electromagnetics and Mechanics,* 49, 453–461.

Wrobel, W., Fornalik-Wajs, E., Szmyd, J.S. (2010) "Experimental and numerical analysis of thermo-magnetic convection in a vertical annular enclosure," *Int. J. Heat Fluid Flow* 31, 1019–1031.